Transport coefficients of QCD from Kubo formalism

Armen Sedrakian
IPT, Wroclaw University
Frankfurt Institute for Advanced Studies

Wroclaw, 11 October, 2019

Outline

QCD phase diagram

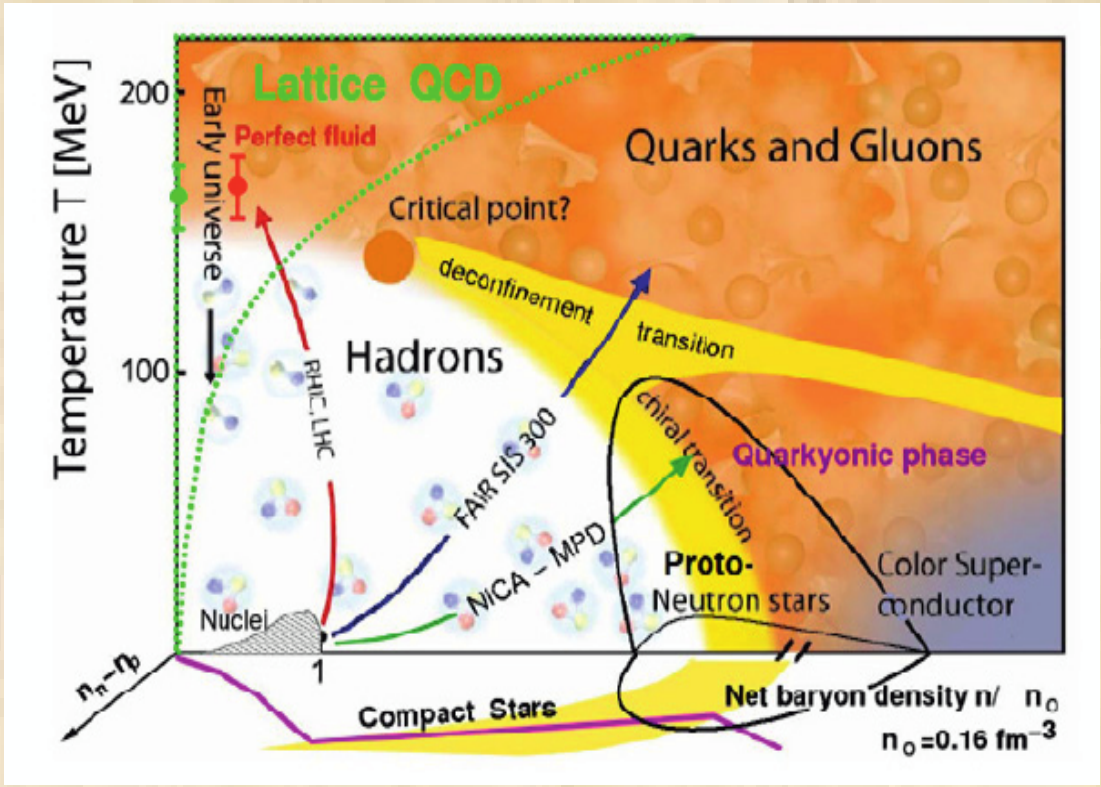

Methods to explore phases of QCD

1. Low-energy sector - chiral perturbation theory
2. High temperatures and/or high densities - perturbative QCD
3. Finite temperatures and low densities - lattice QCD
4. Intermediate temperature/densities - effective models: NJL model, Dyson-Schwinger

Relativistic heavy-ion collisions

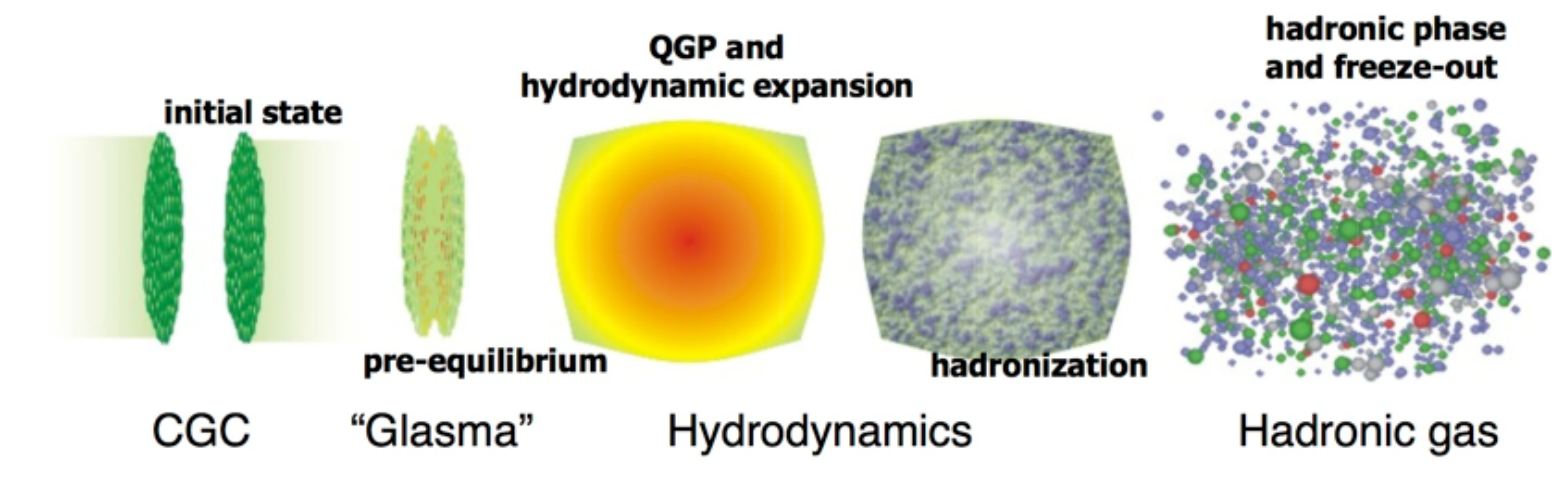

Dynamical stages of ultrarelativistic heavy-ion collisions

1. Pre-equilibrium
   At proper times $\tau \lesssim 1$ fm after the collision the distribution of particle momenta in the expanding fireball of QGP is not thermal.

2. Thermalization and hydrodynamic flow
   At time scales $1 \lesssim \tau \lesssim 4$ fm local thermal equilibrium is achieved, and the evolution of QGP can be described by relativistic fluid dynamics.

3. Hadronization and freeze-out
   At $\tau \gtrsim 5$ fm QGP undergoes a phase transition to the hadronic phase and goes out of equilibrium. In this stage the particle flows should be described by kinetic theory.

Fluid dynamics is an effective theory which describes collective phenomena in many-particle systems in low-frequency and long-wave-length limit.

- Relativistic fluids are described completely by the energy-momentum tensor $T^{\mu\nu}$ and conserved particle 4-current N^μ – 14 variables

$$\partial_\mu T^{\mu\nu} = 0, \qquad \partial_\mu N^\mu = 0 \qquad - \qquad \text{5 equations.} \qquad (1)$$

- $T^{\mu\nu}$ and N^μ can be decomposed as ($\Delta_{\mu\nu} = g_{\mu\nu} - u_\mu u_\nu$)

$$T^{\mu\nu} = \underbrace{\epsilon u^\mu u^\nu - p\Delta^{\mu\nu}}_{\textit{ideal part}} \underbrace{- \Pi\Delta^{\mu\nu} + \pi^{\mu\nu} + q^\mu u^\nu + q^\nu u^\mu}_{\textit{dissipative part}}, \qquad N^\mu = \underbrace{nu^\mu}_{\textit{id.}} + \underbrace{J^\mu}_{\textit{diss.}}$$

- We have the following dissipative quantities

Π	–	bulk viscous pressure	(1 component)
$\pi^{\mu\nu}$	–	shear stress tensor	(5 components)
q^μ	–	energy diffusion flux	(3 components)
J^μ	–	particle diffusion flux	(3 components)

Landau frame: $q^\mu = 0$; Eckart frame: $J^\mu = 0$ $\Rightarrow$ 9 variables

- To close the system (1) one needs an **equation of state $p = p(\epsilon, n)$** + **9 transport equations** for the dissipative quantities.

Dissipative fluid dynamics

1. **Ideal fluid dynamics**
   Based on the assumption of *local thermal equilibrium*
   $\Rightarrow$ no dissipation: $\Pi = \pi^{\mu\nu} = q^{\mu} = J^{\mu} = 0$.
2. **Relativistic Navier-Stokes (first-order) theory**
   Linear constitutive relations beween dissipative fluxes and thermodynamic forces
   $\Rightarrow$ suffers from acausality and numerical instability.

Various methods to derive transport equations and transport coefficients

- Kinetic theory: based on the Boltzmann equation for the quasiparticle distribution function $\Rightarrow$ applicable for *systems with well-defined quasiparticles*.
- **Kubo-Zubarev formalism**: based on the generalization of the Gibbs canonical ensemble for non-equilibrium states $\Rightarrow$ applicable for *strongly interacting systems*.
- Holographic methods: based on fluid/gravity duality $\Rightarrow$ applicable for certain class of field theories in the *limit of infinitely strong coupling*.

D. Zubarev, *Nonequilibrium Statistical Thermodynamics*, Studies in Soviet science. Consultants Bureau (1974).
D. Zubarev, V. Morozov and G. Röpke, *Statistical Mechanics of Nonequilibrium Processes*, John Wiley & Sons (1997).

Local equilibrium statistical operator

- Thermodynamics of quantum systems is described via the statistical operator $\hat{\rho}(t)$ (density matrix), which in thermal equilibrium is given by the Gibbs distribution

$$\hat{\rho}_{\rm eq} = Z^{-1} \exp\Big[-\beta\Big(\hat{H} - \mu\hat{\mathcal{N}}\Big)\Big].$$

- In an arbitrary reference frame we replace $\hat{H} \to \hat{\mathcal{P}}_\nu u^\nu$, and substitute

$$\hat{\mathcal{P}}_\nu = \int d^3x \hat{T}_{0\nu}(x), \qquad \hat{\mathcal{N}} = \int d^3x \hat{N}_0(x).$$

- The Lorentz-covariant form of the Gibbs distribution reads ($x \equiv (\boldsymbol{x}, t)$)

$$\hat{\rho}_{\rm eq} = Z^{-1} \exp\Big\{ -\int d^3x \beta\Big[u^\nu \hat{T}_{0\nu}(x) - \mu\hat{N}_0(x)\Big]\Big\}.$$

- In *local thermal equilibrium* $\beta \to \beta(x)$, $\mu \to \mu(x)$, $u_\mu \to u_\mu(x)$, and

$$\hat{\rho}_{\rm eq}(\beta, \mu, u_\mu) \to \hat{\rho}_l\Big[\beta(x), \mu(x), u_\mu(x)\Big].$$

Local equilibrium distribution cannot describe irreversible processes!

Solving the Liouville equation

The NESO $\hat{\rho}(t)$ should be found from the Liouville equation (Heisenberg picture)

$$\frac{d\hat{\rho}(t)}{dt} = 0. \qquad \textbf{time-reversible!}$$

1. Imposing an initial condition $\hat{\rho}(t_0) = \hat{\rho}_l(t_0)$, we find a formal solution

$$\hat{\rho}(t) = \hat{\rho}_l(t_0), \qquad t \geq t_0.$$

2. The required *irreversible* solution for NESO can be obtained by averaging the solution above over all possible initial states from $-\infty < t_0 < t$

$$\hat{\rho}(t) = \lim_{T\to\infty} \frac{1}{T} \int_{-T}^{t} dt_0\, \hat{\rho}_l(t_0) = \lim_{\varepsilon\to+0} \varepsilon \int_{-\infty}^{t} dt_0\, e^{\varepsilon(t_0-t)}\, \hat{\rho}_l(t_0),$$

where we used Abel's theorem.

This operator satisfies the Liouville equation with an infinitesimal source term

$$\frac{d\hat{\rho}(t)}{dt} = -\lim_{\varepsilon\to+0} \varepsilon\, [\hat{\rho}(t) - \hat{\rho}_l(t)]. \qquad \textbf{time-irreversible!}$$

Non-equilibrium statistical operator

Now the full NESO can be written as

$$\hat{\rho}(t) = Q^{-1} e^{-\hat{A}+\hat{B}}, \qquad Q = \mathrm{Tr} e^{-\hat{A}+\hat{B}},$$

where

$$\hat{A}(t) = \int d^3x \left[\beta^\nu(x) \hat{T}_{0\nu}(x) - \alpha(x) \hat{N}_0(x) \right]$$

is the local equilibrium part with $\beta^\nu = \beta u^\nu$, $\alpha = \beta\mu$, and

$$\begin{aligned} \hat{B}(t) &= \lim_{\varepsilon \to +0} \int d^3x_1 \int_{-\infty}^{t} dt_1 \, e^{\varepsilon(t_1 - t)} \, \hat{C}(x_1), \\ \hat{C}(x) &= \hat{T}_{\mu\nu}(x) \partial^\mu \beta^\nu(x) - \hat{N}_\mu(x) \partial^\mu \alpha(x). \end{aligned}$$

The operator $\hat{B}$ is a thermodynamic "force" as it involves the gradients of β, μ and u_μ. Naturally, it can be identified with the non-equilibrium part of the statistical operator.

If $\hat{B} = 0$, we recover the local equilibrium statistical operator

$$\hat{\rho}_l(t) = Q_l^{-1} e^{-\hat{A}}, \qquad Q_l = \mathrm{Tr} e^{-\hat{A}}.$$

Statistical averages and correlation functions

- Now we treat the non-equilibrium part $\hat{B}$ of the NESO as a perturbation

$$\hat{\rho} = \hat{\rho}_l + \hat{\rho}_1 + \dots .$$

- Statistical average of any operator $\hat{X}(x)$ can be written as

$$\langle \hat{X}(x) \rangle = \mathrm{Tr}[\hat{\rho}(t)\hat{X}(x)] = \langle \hat{X}(x) \rangle_l + \langle \hat{X}(x) \rangle_1 + \dots ,$$

where

$$\langle \hat{X}(x) \rangle_1 \quad = \quad \int d^4x_1 \left(\hat{X}(x), \hat{C}(x_1) \right) + \dots$$

- The two-point correlation function is related to the retarded Green's function

$$\left(\hat{X}(x), \hat{C}(x_1) \right) = -\frac{1}{\beta} \int_{-\infty}^{t_1} dt' \; G^R_{\hat{X}\hat{C}}(\boldsymbol{x} - \boldsymbol{x}_1, t - t').$$

Matching conditions

- The fluid 4-velocity u_μ should be connected to one of the physical currents.

  1. Landau-Lifshitz frame: u_μ is connected to the energy flow

  $$u_\mu \langle \hat{T}^{\mu\nu} \rangle = \langle \hat{\epsilon} \rangle u^\nu, \qquad \text{where} \qquad \hat{\epsilon} = u_\mu u_\nu \hat{T}^{\mu\nu}.$$

  2. Eckart frame: u_μ is connected to the particle flow

  $$\langle \hat{N}^\mu \rangle = \langle \hat{n} \rangle u^\mu, \qquad \text{where} \qquad \hat{n} = u_\mu \hat{N}^\mu.$$

- The temperature and chemical potential are well-defined only in full thermal equilibrium. In non-equilibrium they are defined via the following matching conditions

$$\langle \hat{\epsilon}(x) \rangle = \langle \hat{\epsilon}(x) \rangle_l, \qquad \langle \hat{n}(x) \rangle = \langle \hat{n}(x) \rangle_l.$$

Navier-Stokes limit of the transport equations

- The thermodynamic force to the first-order in gradients can be decomposed as

$$\hat{C} = -\beta\hat{p}^*\theta + \beta\hat{\pi}_{\mu\nu}\sigma^{\mu\nu} - \left(\hat{J}_\mu - \frac{n}{h}\hat{q}_\mu\right)\nabla^\mu\alpha,$$

  where $\theta = \partial_\mu u^\mu$, $\nabla_\mu = \Delta_{\mu\nu}\partial^\nu$, $\sigma_{\mu\nu} = \nabla_{\langle\alpha}u_{\beta\rangle}$.
- In this approximation we obtain the relativistic NS equations (Landau frame)

$$\Pi = -\zeta\theta, \qquad \pi_{\mu\nu} = 2\eta\sigma_{\mu\nu}, \qquad J_\mu = \chi\nabla_\mu\alpha.$$

- Three (first-order) transport coefficients:

$$\begin{aligned} \zeta &- \text{bulk viscosity} \\ \eta &- \text{shear viscosity} \\ \chi &- \text{diffusion coefficient} \\ \kappa = \left(\frac{\epsilon+p}{nT}\right)^2\chi &- \text{thermal conductivity} \end{aligned}$$

- Navier-Stokes equations imply **instantaneous** response of dissipative fluxes to thermodynamic

The QGP phase of heavy ion collisions are well described by hydrodynamics – dissipative effects are accounted in terms of transport coefficients

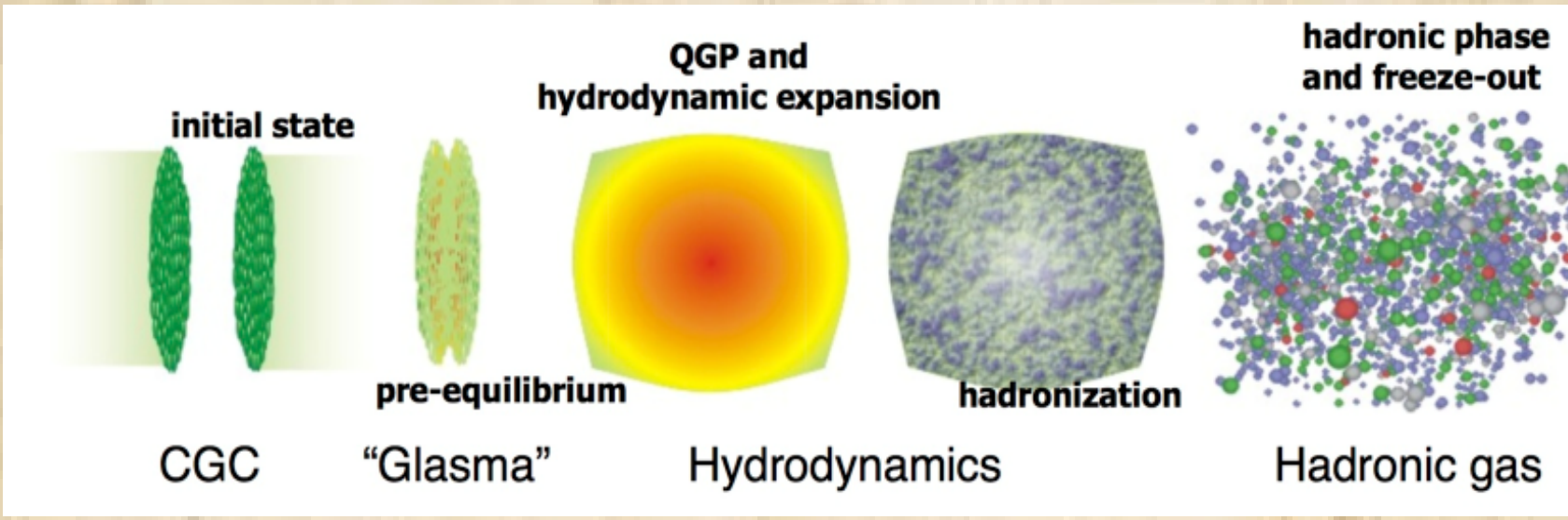

Fits to elliptic flow suggest low viscosity close to the universal bound

$$\frac{\eta}{s} \geq \frac{1}{4\pi}$$

Fluid dynamics works surprisingly well for heavy ion collisions in the range of energies at RHIC and LHC!

Methods for transport coefficients

1. Linearized Boltzmann Equation: applicable for weakly interacting systems and e.g. Fermi-liquids (quasiparticles) not far from equilibrium
2. Direct numerical solutions of the Boltzmann equation: typically little insight and control over approximations
3. Real-time evolution of propagators (Kadanoff-Baym): truncation of self-energies, numerically complex problem, but valid far from equilibrium (beyond hydrodynamics)
4. Imaginary time Kubo formalism - relates two-point correlation functions to transport coefficients, valid in principle for *strongly correlated system.*

The method of non-equilibrium statistical operator developed by D. N. Zubarev (1974).

X.-G. Huang, A. Sedrakian, D. H. Rischke,
Kubo formulae for relativistic fluids in strong magnetic fields.
Annals of Physics (NY) 326, 3075 (2011).
A. Harutyunyan and A. Sedrakian,
Bulk viscosity of two-flavor quark matter from the Kubo formalism.
Phys. Rev. D **96**, 034006 (2017). Particles 2018, **1(1)**, 212-229.
A. Harutyunyan, D. H. Rischke and A. Sedrakian,
Transport coefficients of two-flavor quark matter from the Kubo formalism.
Phys. Rev. D **95**, 114021 (2017). Particles 2018, **1,** 11

Kubo formulae

Relations between the transport coefficients and correlation functions

$$\kappa = -\frac{\beta}{3}\frac{d}{d\omega}\mathrm{Im}\Pi^R_\kappa(\omega)\Big|_{\omega=0}, \quad \Pi^R_\kappa(\omega) = i\int_0^\infty dt\, e^{i\omega t}\int d\boldsymbol{r}\langle[q_\mu(\boldsymbol{r},t), q^\mu(0)]\rangle_0,$$

$$\sigma = -\frac{1}{3}\frac{d}{d\omega}\mathrm{Im}\Pi^R_\sigma(\omega)\Big|_{\omega=0}, \quad \Pi^R_\sigma(\omega) = i\int_0^\infty dt\, e^{i\omega t}\int d\boldsymbol{r}\langle[j_\mu(\boldsymbol{r},t), j^\mu(0)]\rangle_0,$$

$$\eta = -\frac{1}{10}\frac{d}{d\omega}\mathrm{Im}\Pi^M_\eta(\omega)\Big|_{\omega=0}, \quad \Pi^R_\eta(\omega) = -i\int_0^\infty dt\, e^{i\omega \tau}\int d\boldsymbol{r}\langle[\pi_{\mu\nu}(\boldsymbol{r},\tau), \pi^{\mu\nu}(0)]\rangle_0,$$

with $\pi_{\mu\nu}$ being the shear viscosity tensor and thermal and electrical currents defined as

$$\pi_{\mu\nu} = \Delta^{\alpha\beta}_{\mu\nu}T_{\alpha\beta}, \quad q_\mu = \Delta_{\mu\alpha}u_\beta T^{\alpha\beta} - h\Delta_{\mu\alpha}N^\alpha,$$
$$j_\mu = \Delta_{\mu\alpha}J^\alpha, \qquad J_\mu = \bar\psi\hat{Q}\gamma_\mu\psi, \quad \Delta_{\mu\nu} = g_{\mu\nu} - u_\mu u_\nu.$$

h is the enthalpy per particle.

The two-flavor Nambu-Jona-Lasinio Lagrangian

Consider two-flavor quark matter described by by the NJL Lagrangian with scalar ($\Gamma = 1$) and pseudoscalar-isovector ($\Gamma = i\gamma_5\vec{\tau}$)

$$\boxed{\mathcal{L} = \bar{\psi}(i\partial\!\!\!/ - m_0)\psi + \frac{G}{2}\left[(\bar{\psi}\psi)^2 + (\bar{\psi}i\gamma_5\boldsymbol{\tau}\psi)^2\right],}$$

Advantages: NJL has all global symmetries of QCD: $SU_V(2) \times SU_A(2) \times U_V(1)$. It features chiral symmetry breaking with pions emerging as the Goldstone modes.
Shortcomings: NJL does not confine at low energies. It is non-renormalizable, and a momentum cutoff ($p \leq \Lambda$) is applied to regularize the ultraviolet divergences.

Input parameters: $m_0 = 5.5$ MeV, $G = 10.1$ GeV, $\Lambda = 650$ MeV,
Output parameters: $m = 325$ MeV, $m_\pi = 140$ MeV, $f_\pi = 92.4$ MeV,

The energy-momentum tensor, particle current and electric current read as

$$T_{\mu\nu} = \frac{i}{2}(\bar{\psi}\gamma_\mu\partial_\nu\psi + \bar{\psi}\gamma_\nu\partial_\mu\psi) - g_{\mu\nu}\mathcal{L}, \quad N_\nu = \bar{\psi}\gamma_\nu\psi, \quad J_\mu = \bar{\psi}\hat{Q}\gamma_\mu\psi$$

where $\hat{Q}$ is the charge matrix for u and d quarks.

Quark masses

Quasiparticle propagators of quarks are given by

$$S(\boldsymbol{p},\omega_m) = \frac{\Lambda_p^+\gamma_0}{i\omega_m - E_p} + \frac{\Lambda_p^-\gamma_0}{i\omega_m + E_p}$$

Dynamically generated (Hartree) mass is given by

$$m = m_0 + G\langle\bar\psi\psi\rangle, \quad \langle\bar\psi\psi\rangle = -\frac{mN_cN_f}{\pi^2}\int_0^\Lambda dp\frac{p^2}{E_p}[1 - n^+(E_p) - n^-(E_p)].$$

Diagrammatically the dynamically generated mass is given by

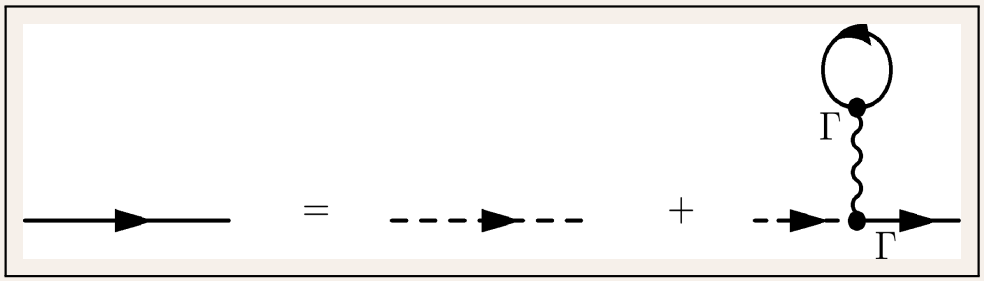

Mesons masses

The meson propagators are obtained from the Bethe-Salpeter equation

$$D_M = G + G\Pi_M D_M = \frac{G}{1 - G\Pi_M}, \quad D_M(p_0, \boldsymbol{p}) = \frac{-g_M^2}{p_0^2 - \boldsymbol{p}^2 - m_M^2 + i\epsilon}$$

where the quark-antiquark polarizations for sigma meson and pion $\Pi_M, M = \sigma, \pi$ are given by the formula

$$\Pi_M(\boldsymbol{p}, \omega_n) = -T \sum_{m \in Z} \int \frac{d\boldsymbol{q}}{(2\pi)^3} \mathrm{Tr}[\Gamma_M S(\boldsymbol{q} + \boldsymbol{p}, \omega_m + \omega_n) \Gamma_M S(\boldsymbol{q}, \omega_m)]$$

with $\Gamma_\sigma = 1, \Gamma_\pi = i\gamma_5 \tau_j, j = 1, 2, 3.$

Diagrammatically the meson propagator is given by

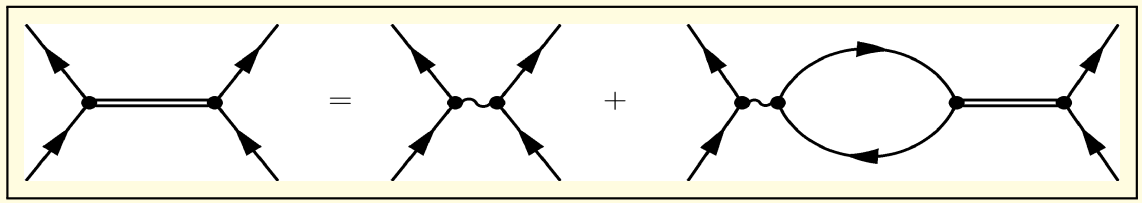

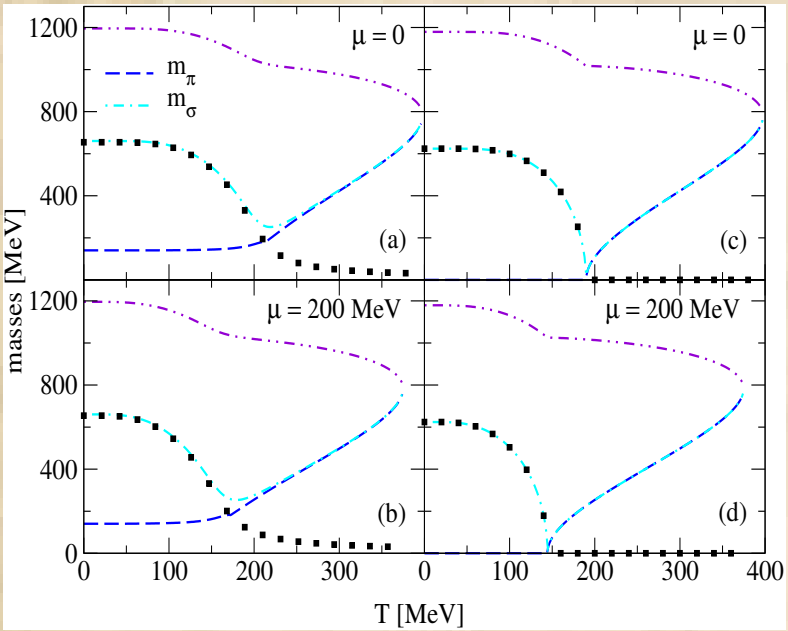

The quark and meson masses; the dotted lines show twice the quark mass. The right panels correspond to the chiral limit $m_0 = 0$.

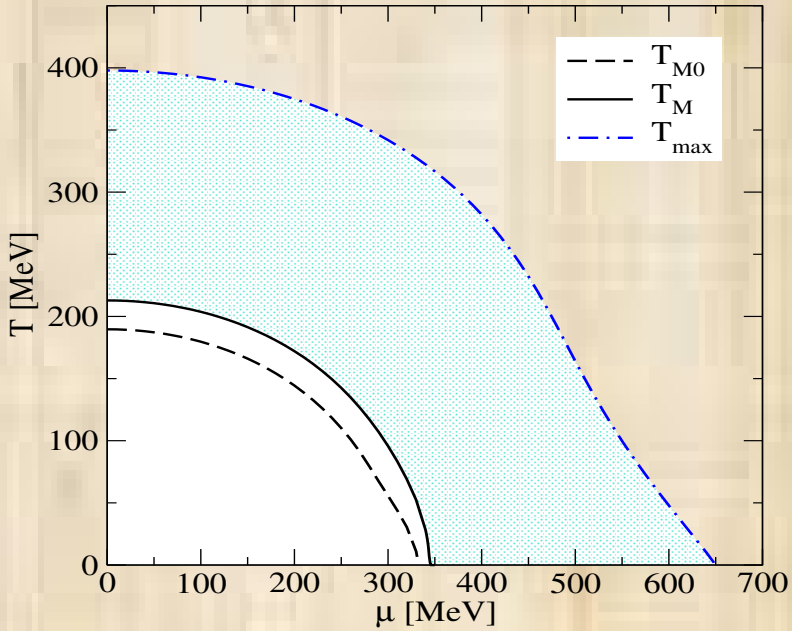

The Mott temperature T_{M} - solid and chiral counterpart - dashed as well as the temperature $T_{\max}$ as functions of the chemical potential.

The computation of transport coefficients is relevant to the shaded area, i.e., between the Mott line and the maximal temperature where the solutions for meson masses are found.

Power counting scheme for NJL Lagrangian

- each loop gives a factor N_c which arises from the trace in the color space
- each coupling G (which is associated with a pair of $\Gamma^0_{s/ps}$ matrices) gives $1/N_c$
- for any given number of $\Gamma^0_{s/ps}$ vertices the leading diagram in $1/N_c$ approximation is the one that has the maximum number of loops
- second line type diagram vanish for (a) pseudoscalar vertices due to the trace in the Dirac space, (b) for scalar vertices the integrand is odd in momentum

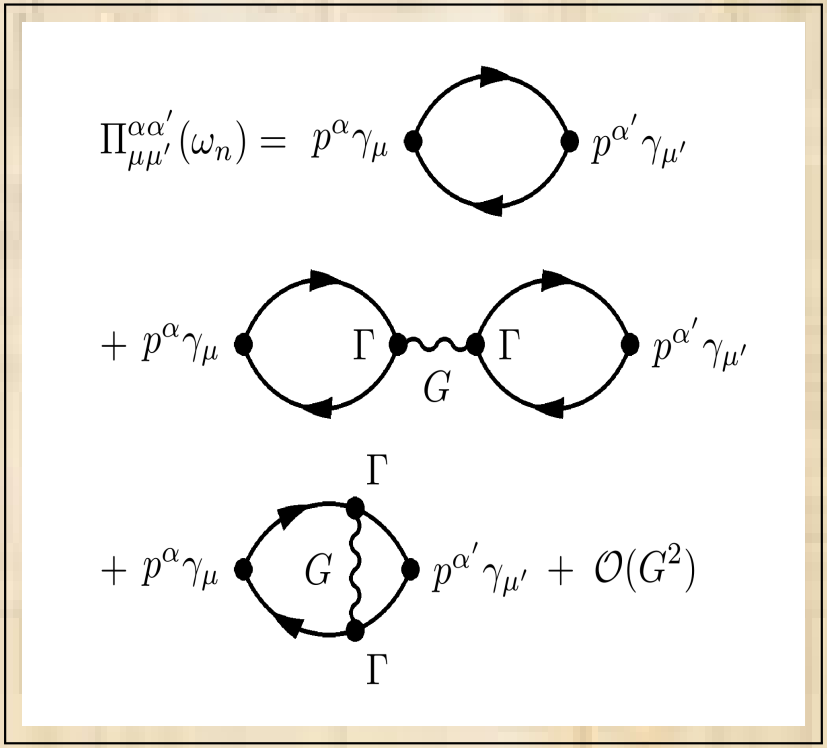

Bottom line: In $1/N_c$ counting scheme the leading order diagram is given by the single loop with full propagators.

The dominant process: meson decays into two quarks and its inverse for $T > T_M$

$$\Sigma^M(\boldsymbol{p},\omega_n) \quad = \quad$$

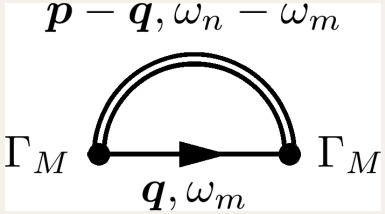

$$= T\sum_m \int \frac{d\boldsymbol{q}}{(2\pi)^3}\left[\Gamma_M S(\boldsymbol{q},\omega_m)\Gamma_M D_M(\boldsymbol{p}-\boldsymbol{q},\omega_n-\omega_m)\right],$$

the index $M=\pi,\sigma$ indicates the meson and $\Gamma_\sigma = 1$ and $\Gamma_\pi = i\gamma_5\boldsymbol{\tau}$

Decomposition of the self-energy is given by

$$\Sigma^M(\boldsymbol{p},\omega_n) = P_M m\Sigma_s^M + i\omega_n\gamma_0\Sigma_0^M - \boldsymbol{p}\boldsymbol{\gamma}\Sigma_v^M,$$

where $P_\sigma = 1, P_\pi = -1$ (parity conservation, translational and rotational invariance, time-reversal invariance). The three components of spectral function

Analogous decomposition of the spectral function is given

$$A(p_0,\boldsymbol{p}) \quad = \quad -\frac{1}{\pi}(mA_s + p_0\gamma_0 A_0 - \boldsymbol{p}\boldsymbol{\gamma}A_v).$$

Transport coefficients

$$\kappa = -\frac{N_c N_f}{6\pi^3 T}\int_{-\infty}^{\infty} d\varepsilon \frac{\partial n}{\partial \varepsilon}\int_0^{\Lambda} dp p^2 \Big\{ \left[A_s^2(p,\varepsilon)m^2 - A_0^2(p,\varepsilon)\varepsilon^2 + A_v^2(p,\varepsilon)p^2\right] \times \left[p^2 - 3(\varepsilon-2h)^2\right] + 2\left[A_0(p,\varepsilon)\varepsilon + A_v(p,\varepsilon)(\varepsilon-2h)\right]^2 p^2 \Big\},$$

$$\sigma = \frac{40 N_c \alpha}{27\pi^2}\int_{-\infty}^{\infty} d\varepsilon \frac{\partial n}{\partial \varepsilon}\int_0^{\Lambda} dp p^2 \left[3A_s^2(p,\varepsilon)m^2 - 3A_0^2(p,\varepsilon)\varepsilon^2 + A_v^2(p,\varepsilon)p^2\right],$$

$$\eta = \frac{N_c N_f}{15\pi^3 T}\int_{-\infty}^{\infty} d\varepsilon \frac{\partial n}{\partial \varepsilon}\int_0^{\Lambda} dp\, p^4 \left[5A_s^2(p,\varepsilon)m^2 - 5A_0^2(p,\varepsilon)\varepsilon^2 + A_v^2(p,\varepsilon)p^2\right],$$

and combinations

$$\frac{\eta}{s} \geq \frac{1}{4\pi} \quad \text{(KSS bound)} \qquad \frac{\kappa}{\sigma} \propto T \quad \text{(Wiedemann} - \text{Franz law)}$$

Lorentz components of the imaginary part of the quark self-energy

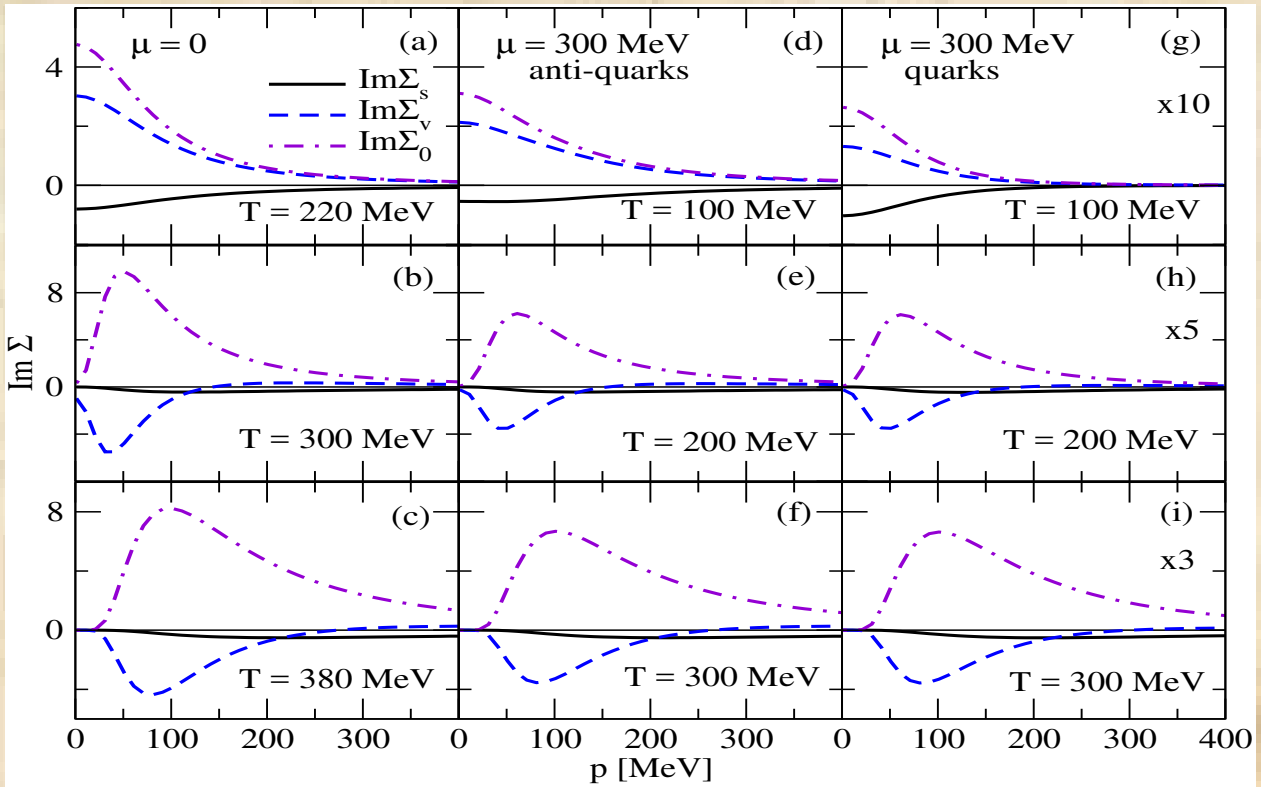

- Small-p asymptotics is different for $(m_M^2 - 2m^2)/2m > T$ and $< T$; in the first case contributions are not suppressed, in the second case they are.
- In the large-p limit the integration range is broad and this asymptotics is controlled by the statistical effects (the cut-off by the distribution functions of the high-momentum contributions)
- At the same time the distribution functions cover phase space with higher energies. Combined this leads to an increase of the imaginary parts of self-energies of quarks and anti-quarks with temperature, which is well pronounced for high momenta.

Lorentz components of the spectral functions of quarks, which are shown at three energies $\varepsilon_1 = 100$, $\varepsilon_2 = 300$, and $\varepsilon_3 = 500$ MeV.

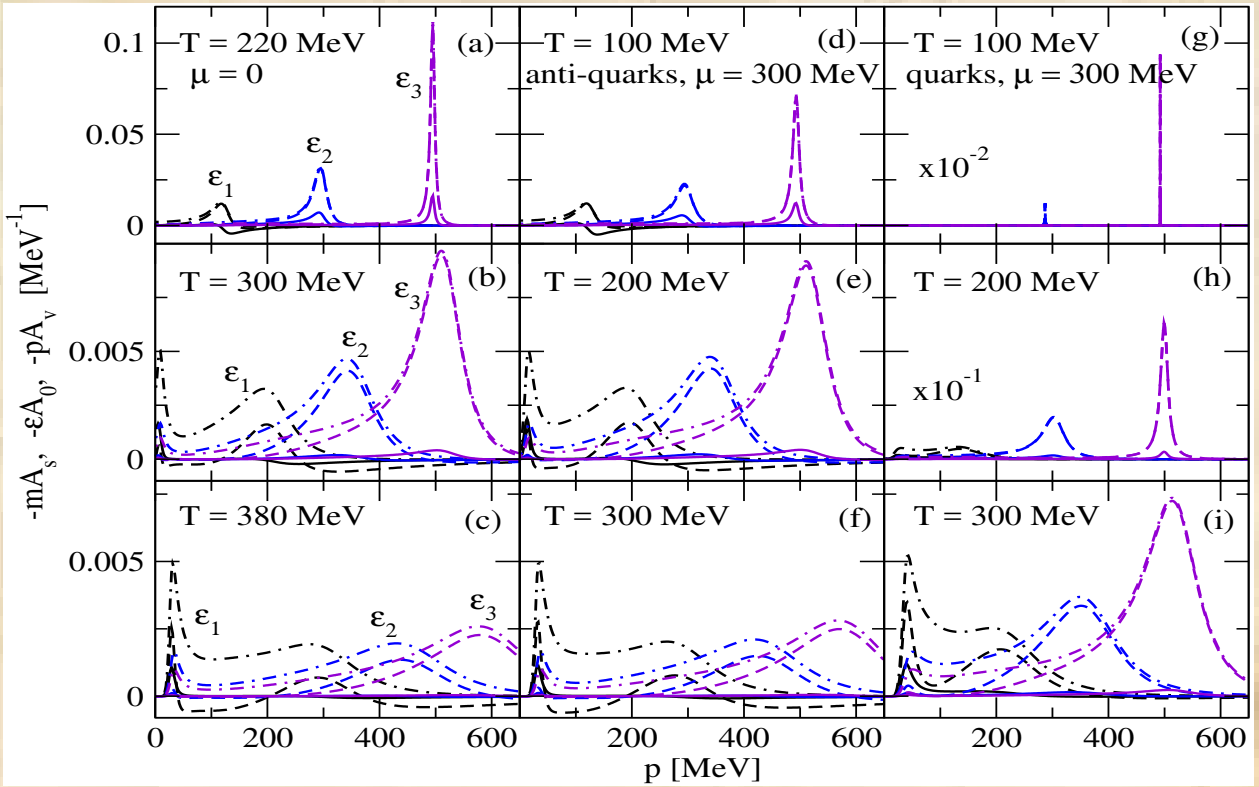

- The quasiparticle peak in the spectral functions appears for $p \simeq \varepsilon$.
- In all cases it is seen that the height of peaks increases with the quark energy.
- The quasiparticle peaks are broadened with increasing temperature and are replaced by more complex structures in the high temperature regime, see (c)-(f)-(i).

Dependence on T/T_M.

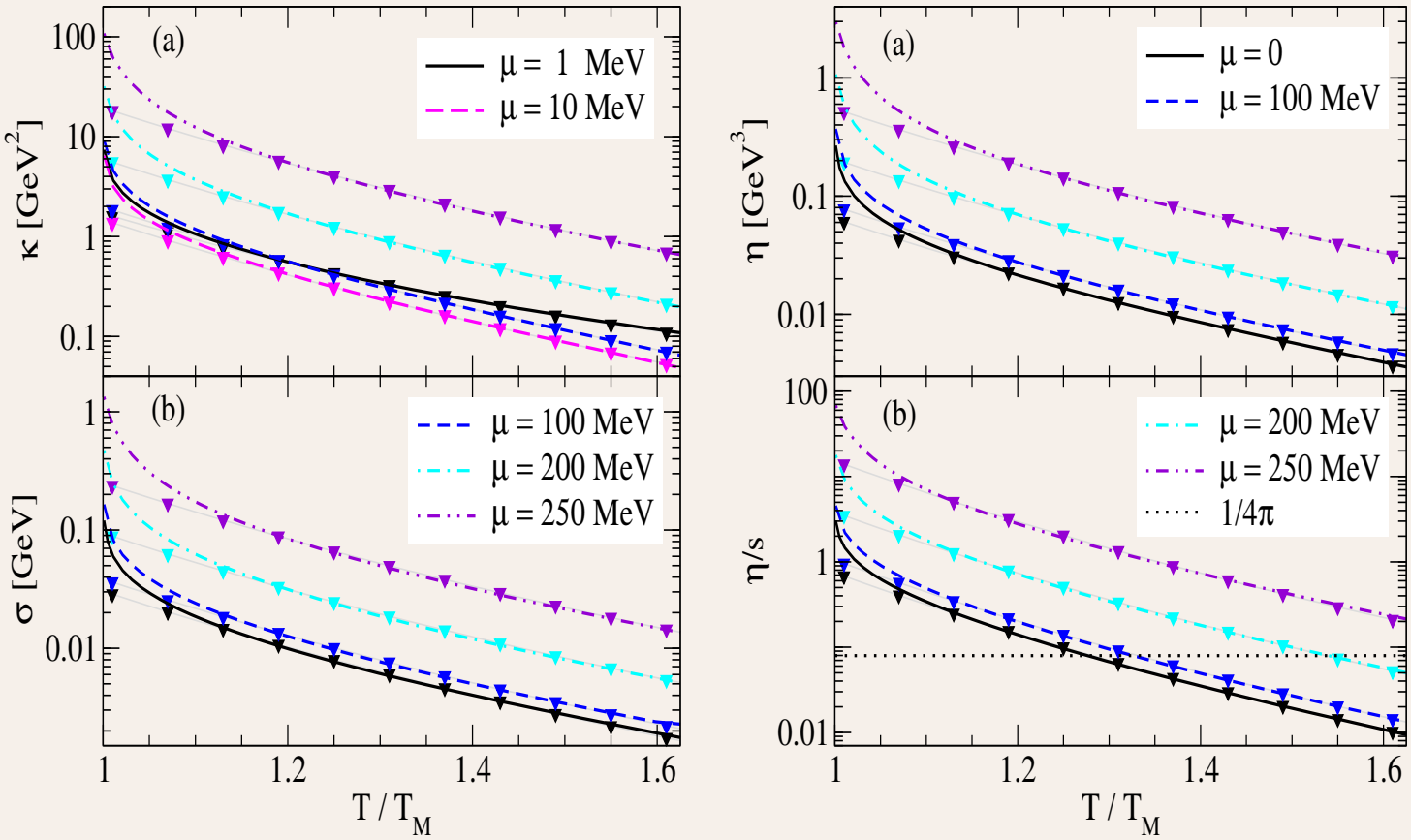

- To remove the effect of the variations of the position of the Mott line with the chemical potential, we show the conductivities with the temperature axis scaled by corresponding $T_{\mathrm{M}}(\mu)$.
- The conductivities (the convergent part in the case of κ) display a universal dependence on this scaled temperature, their values being only shifted by a μ-dependent constant.

Dependence on μ

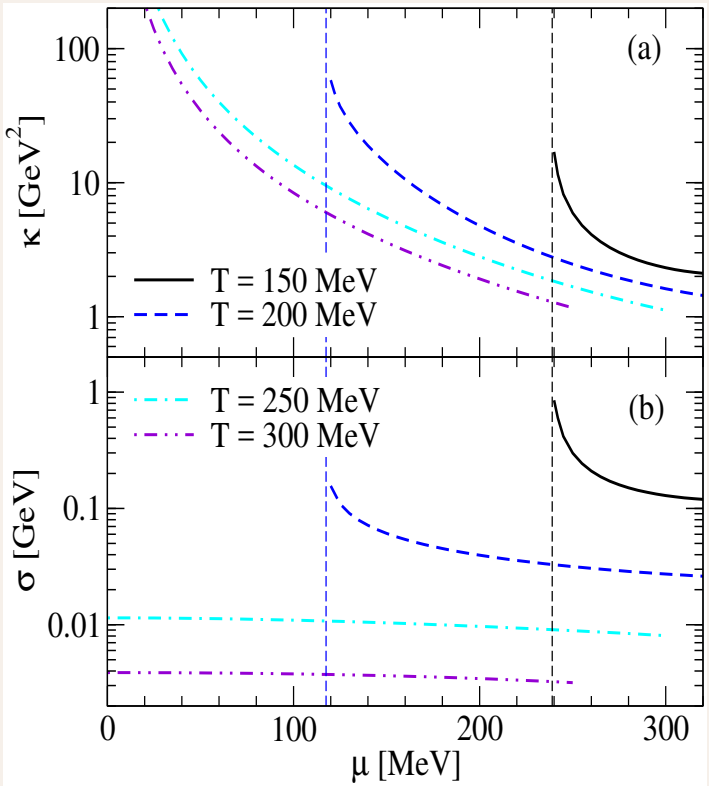

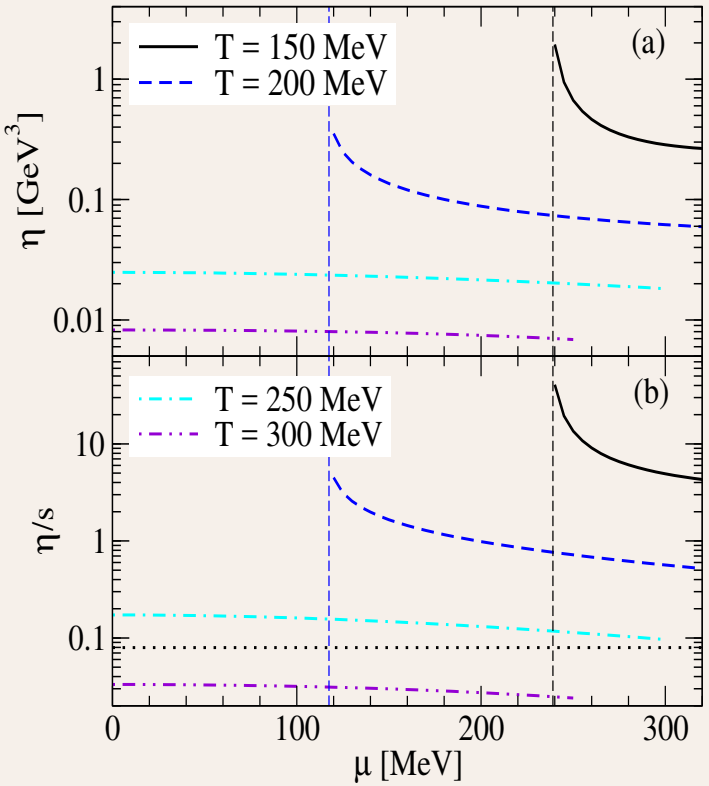

- The conductivities are nearly independent of the chemical potential away from the Mott transition line.
- Only close to this transition the conductivities increase because of the vanishing of the spectral width.

Fits to our results

Fit formulae for the numerical results

- Fit the Mott transition line

$$T_{\rm M}^{\rm fit}(\mu) = T_0 \begin{cases} 1 - \sqrt{\gamma y} e^{-\pi/(\gamma y)} & 0 \le y \le 0.5, \\ \sqrt{1.55(1-y) + 0.04(1-y)^2} & 0.5 < y \le 1, \end{cases}$$

  $y = \mu/\mu_0$, where $\mu_0 = 345$ MeV.

- All the transport coefficient can be fitted with a generic formula

$$\chi_{\rm fit} = C \left(\frac{T}{T_{\rm M}}\right)^{-\alpha} \exp[a_1 y + a_2 y^2 + a_3 y^3], \quad \chi_{\rm fit} \in \{\sigma, \kappa, \eta, \eta/s\}.$$

- The fit parameters are given by

$\chi_{\rm fit}$	C	α	a_1	a_2	a_3
σ	0.0305	6	2.64	1.23	2.67
κ	0.3130	6	2.90	1.0	2.63
η	0.129	6	2.77	1.16	2.54
η/s	1.49	9	3.89	1.72	3.47

Gluons are important for the large temperatures

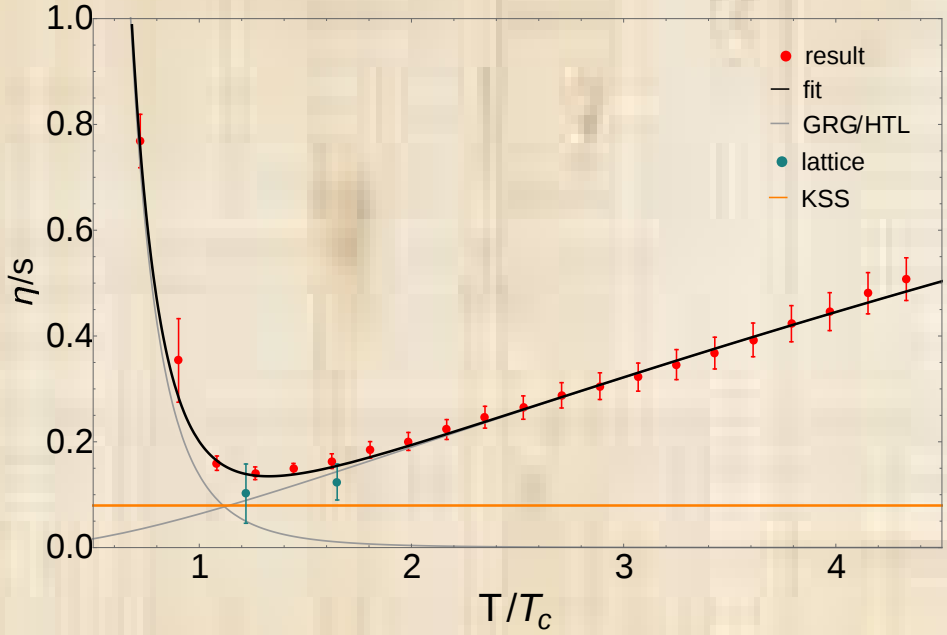

adapted from N. Christiansen et al, arXiv:hep-ph 1411.

Conclusions on transport coefficients

- Obtained Kubo formulae from Zubarev formalism for the electrical and thermal conductivities of relativistic quark plasma taking into account the full Lorentz structure of the self-energies (spectral functions) of the quarks.
- Our Kubo formulae for conductivities have generic validity and can be applied in a broader context of field theories of relativistic plasmas, in a straightforward manner when the vertex corrections are suppressed.
- The conductivities are decreasing functions of temperature at fixed chemical potential; they show nearly universal behavior when temperature is scaled by the Mott temperature, i.e. as a function of $T/T_{\rm M}$.
- Provided simple fit formulae for the electrical and thermal conductivities with a good relative accuracy which can be utilized in numerical simulations of magneto-hydrodynamics of quark plasma.